

## Rational Determination of Transfer Free Energies of Small Drugs across the Water–Oil Interface

Delphine Bas,<sup>†</sup> Delphine Dorison-Duval,<sup>‡</sup> Stéphanie Moreau,<sup>‡</sup> Pierre Bruneau,<sup>‡</sup> and Christophe Chipot<sup>\*,†</sup>

*Equipe de chimie théorique, UMR CNRS/UHP 7565, Institut nancéien de chimie moléculaire, Université Henri Poincaré, BP 239, 54506 Vandœuvre-lès-Nancy Cedex, France, and ASTRAZENECA, Centre de recherche, Z. I. La Pompelle, BP 1050, 51689 Reims Cedex 2, France*

Received June 26, 2001

The application of statistical simulations to the estimation of transfer free energies of pharmacologically relevant organic molecules is reported. Large-scale molecular dynamics simulations have been carried out on a series of four solutes, viz. antipyrine, caffeine, ganciclovir, and  $\alpha$ -D-glucose, at the water–dodecane interface as a model of a biological water–membrane interfacial system. Agreement with experimentally determined partition coefficients is remarkable, demonstrating that free energy calculations, when executed with appropriate protocols, have reached the maturity to predict thermodynamic quantities of interest to the pharmaceutical world. The computational effort that warrants accurate, converged free energies remains, however, in large measure, incompatible with the high-throughput exploration of large sets of pharmacologically active drugs sought by industrial settings. Compared to the cost-effective, fast estimation of simple partition coefficients, the present free energy calculations, nevertheless, offer a far more detailed information about the underlying energetics of the system when the solute is translocated across the water–dodecane interface, which can be valuable in the context of de novo drug design.

### 1. Introduction

On the road toward the development of new, pharmacologically active drugs, the notion of bioavailability is of paramount importance, as it governs the natural propensity of a molecule to cross biological barriers such as membranes, and, therefore, reach quantitatively its ultimate target. To a large extent, bioavailability and differential solubility of the molecule in aqueous and organic surroundings are closely related concepts.<sup>1</sup> The full understanding of transfer processes of drugs from a polar medium to a nonpolar one inevitably requires the knowledge of the underlying free energy behavior,<sup>2</sup> arguably the most pertinent thermodynamic quantity here. In particular, addressing the issue of bioavailability in the emerging field of rational, de novo drug design implies apprehending the subtle balance of solute–solvent interactions when the molecule of pharmaceutical interest is transferred from the aqueous environment to the hydrophobic core of the biological membrane.<sup>3–6</sup> In essence, water–membrane partitioning cannot be predicted reliably and accurately without the ability to determine the associated free energy changes. Several attempts to simulate the translocation of small, organic molecules across the water–membrane interface have been reported over the past years.<sup>7–10</sup> Statistical simulations of explicit phospholipid bilayers are, however, computationally demanding—see, for instance, ref 11—which precludes their routine use to estimate transfer free energies of large sets of pharmacologically active drugs. In principle, such calculations give access to the variation in free energy along the complete

pathway, over which the drug is translocated, thereby yielding not only information about its behavior amid the bulk phases, but also in the vicinity of the interface.<sup>10</sup> In sharp contrast, inexpensive computational methods targeted at the determination of partition coefficients<sup>12,13</sup> are only indicative of the distribution of this drug between two media of interest,<sup>14–20</sup> e.g., water and 1-octanol, or water and dodecane. Considering that hydrophobic interactions resulting from the coexistence of two media of different polarity supply the main driving force for the partitioning of the solute into one of the two phases, it is tempting to turn to a more rudimentary model to mimic water–membrane assemblies. One popular approach for investigating the pharmacokinetic properties of drugs consists of employing 1-octanol,<sup>13</sup> the amphipathic nature of which allows the formation of spatial arrangements featuring well-delineated hydrophobic and hydrophilic regions.<sup>21</sup> Alternatively, simple water–hydrocarbon mixtures can be used to represent the abrupt change of polarity between the aqueous environment and the hydrophobic interior of the phospholipid bilayer.<sup>22</sup> In this contribution, a theoretical and experimental synergistic investigation of a series of small, pharmacologically relevant molecules, viz. antipyrine, caffeine, ganciclovir, and  $\alpha$ -D-glucose, at the water–dodecane interface is presented. Interestingly enough, all four compounds are absorbed via transcellular diffusion, the three former undergoing passive translocation, whereas the latter follows a carrier-mediated transport mechanism.<sup>23–25</sup> Large-scale, multi-nanosecond molecular dynamics (MD) have been performed, wherein the free energy for translocating the solutes from the aqueous phase to the nonpolar one was estimated. A unique feature of such first-principles statistical simulations, not accessible to faster ap-

\* Correspondence: chipot@lctn.uhp-nancy.fr. Phone: +33-3-83-91-25-96. Fax: +33-3-83-91-25-30.

<sup>†</sup> Université Henri Poincaré.

<sup>‡</sup> ASTRAZENECA.

proaches aimed at the qualitative estimation of free energy changes, lies in their ability to not only measure partition coefficients but also provide a detailed picture of their interfacial behavior. After describing in the following section the methodological details of the calculations and the experimental measurements carried out, the free energy profiles characterizing the transfer of the four molecules across the water–dodecane interface are discussed and analyzed critically in light of the experimentally determined partition coefficients.

## 2. Methods

**2.1. Description of the System.** Ideally, in the context of de novo rational drug design, it would be desirable to determine a priori the propensity of a molecule of pharmacological interest to translocate through the natural barrier formed by the biological membrane. To this end, the ultimate goal of statistical simulations is to supply in a time-bound fashion accurate free energy profiles characterizing the transfer of that molecule across the water–membrane interface. In sharp contrast with simple partition coefficients, transfer free energy profiles provide a complete view of the underlying energetics involved in the translocation of the solute from the aqueous environment to the hydrophobic core of the bilayer. In particular, they highlight possible barriers implied in the crossing of the dividing surface, or possible interfacial minima resulting from the amphipathic nature of the pharmacologically relevant molecule.<sup>10</sup> For obvious cost-effectiveness reasons, however, atomic-level molecular mechanical simulations of real, phospholipid bilayers remain, to a large extent, incompatible with the already high computational requirements of free energy calculations.<sup>26,27</sup> This is particularly true for industrial settings interested in the exploration of large sets of pharmacologically active molecules within a reasonable time frame. In essence, from an industrial perspective, in silico experiments such as free energy calculations are only viable if they can supply a convincing answer faster than bench experiments would, or, at the least, provide a qualitative answer that is predictive on a rank order basis.

The main difficulty of such statistical simulations lies in the quasi nonergodic behavior of the system when the pharmacologically active molecule is trapped in the headgroup region, requiring massive sampling to yield uniform biased probabilities and, hence, reach convergence of the free energy. Under the assumption that the solute does not interact much with the polar, ionic, or zwitterionic headgroups of the bilayer—which limits the choice of appropriate candidates to nonionic, moderately polar compounds—the water–membrane interface can be modeled by a far simpler chemical system formed by water and a saturated hydrocarbon. In essence, this system retains the key characteristic of the more complex water–membrane assembly, namely the proximity of a polar and a nonpolar medium. The free energy calculations reported hereafter were carried out using a water–dodecane interface. As has been demonstrated recently,<sup>28</sup> water–alkane interfaces constitute convincing models of a water–bilayer system, providing valuable information about the propensity of a drug to cross the biological membrane. It should be noted in passing that earlier studies have brought to light alternative solvents to the widely used 1-octanol, like propylene glycol diphosphate (PGDP),<sup>29</sup> as remarkable candidates for determining partition coefficients. In the present statistical simulations, the transfer of antipyrine, caffeine, ganciclovir, and  $\alpha$ -D-glucose from the aqueous environment to the core of the hydrophobic medium was investigated employing the “umbrella sampling” (US) approach.<sup>30,31</sup>

The system consisted of 74 dodecane chains located between two lamellae of water, each containing 818 molecules. This assembly, thus, involved two water–dodecane interfaces. The dimensions of the simulation box were  $30 \times 30 \text{ \AA}^2$  in the  $x,y$ -plane of the interface and  $200 \text{ \AA}$  in the  $z$ -dimension, perpen-

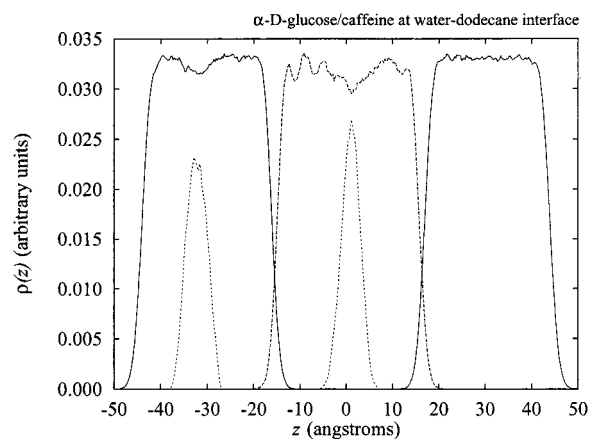


**Figure 1.** Density profiles of caffeine and  $\alpha$ -D-glucose at the water–dodecane interface averaged over 20 000 configurations at 310 K: water (solid line), dodecane (long-dashed line), and solutes (short-dashed line). It should be noted that the presence of the solutes partially disrupts the structure of the liquids, modulating the aspect of the profiles at  $z = -32$  and  $0 \text{ \AA}$ .

dicular to the interface. In this so-called “open” geometry, each water lamella was in equilibrium with its respective vapor phase. In addition to the solvent, the system also contained two solutes—when one was moved from dodecane to water across the first interface, the other was translocated from water to dodecane across the second interface. In such a configuration, the distance separating the solutes is always sufficiently large to warrant that they never interact directly or indirectly (see Figure 1). Periodic boundary conditions were applied in all three directions of space.

Water molecules were described using the TIP4P model.<sup>32</sup> Dodecane chains were represented by the OPLS potential energy function.<sup>33</sup> Bond stretching, valence angle deformation, torsional, and van der Waals parameters of the solutes were extracted from the all-atom AMBER force field of Junmei et al.<sup>34</sup> Net atomic charges were derived from the quantum mechanically calculated molecular electrostatic potential using a self-consistent reaction field (SCRF) approach<sup>35</sup> with an ellipsoidal cavity<sup>36,37</sup> surrounded by a continuum characterized by a macroscopic permittivity of 78.3 (see Figure 2). In doing so, the computed point charges yield a dipole moment appropriate for the aqueous medium, thereby accounting for the missing intermolecular induction effects when the solute is buried in water. In addition, for ganciclovir, which involves a flexible moiety, a “multi-conformational” fitting procedure was utilized,<sup>38</sup> wherein atomic charges were derived to reproduce simultaneously the electrostatic potentials of three distinct conformers. In all cases, the geometries of the solutes were fully optimized in vacuo prior to determining their charge distributions. Quantum chemical calculations were performed at the MP2/6-31G\*\*, MP2/6-311+G\*, MP2/6-31G\*\*, and MP2/6-31G\* for antipyrine, caffeine, ganciclovir, and  $\alpha$ -D-glucose, respectively.

**2.2. Molecular Dynamics Simulations.** All MD simulations were performed in the microcanonical,  $(N, V, \mathcal{E})$ , ensemble.<sup>39</sup> Considering that the system was studied in an “open” geometry, wherein the two water lamellae were in equilibrium with their respective vapor phases, problems connected to an inappropriate adjustment of the pressure, responsible for misrepresented densities, are safely avoided. The SHAKE algorithm<sup>40</sup> was used to constrain the length of the chemical bonds between a hydrogen and a heavy atom. The Newton equations of motion were integrated using the Verlet algorithm with a time-step of  $2 \times 10^{-15} \text{ s}$ . The temperature of the system was maintained at a physiological temperature of 310 K, rescaling periodically the velocities of all particles. Nonbonded interactions were truncated smoothly between 8.5 and  $9.0 \text{ \AA}$ .<sup>41</sup> The rationale for this choice is 2-fold. Comparison of the effects of a smoothed cutoff and the full Coulomb potential in

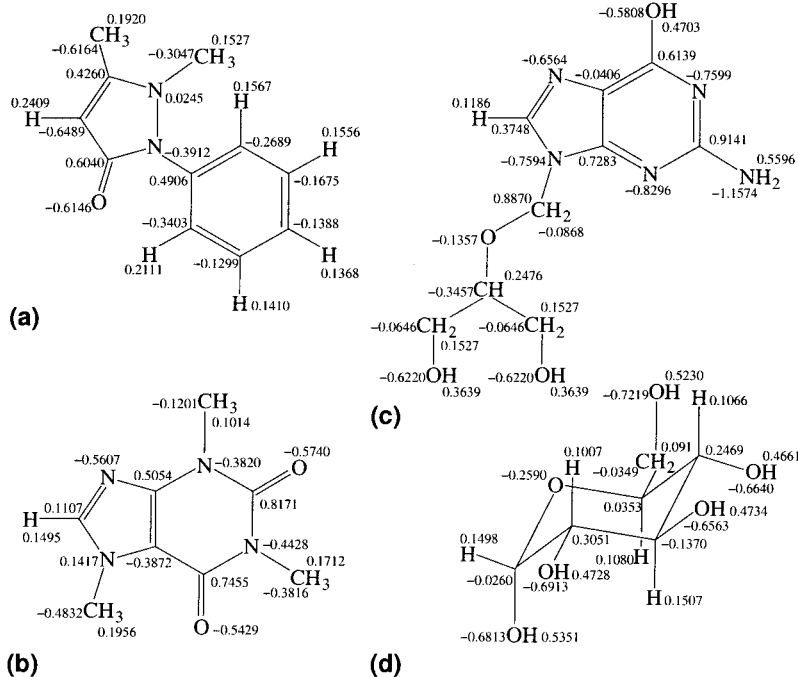


**Figure 2.** Potential derived net atomic charges of antipyrine, caffeine, ganciclovir, and  $\alpha$ -D-glucose determined at the MP2/6-31G\*\*, MP2/6-311+G\*, MP2/6-31G\*\*, and MP2/6-31G\* levels of approximation, respectively, using an SCRf description of the surroundings with a macroscopic permittivity of 78.3.

statistical simulations of polar solutions revealed little changes in their structural and thermodynamic properties.<sup>42</sup> In addition, simulations of moderately polar solutes, using a spherical truncation and a reaction field,<sup>43</sup> indicated that the long-range, electrostatic interactions modulate the free energy of hydration only marginally.

The free energy along the  $z$ -direction, normal to the water–dodecane interface, was calculated using the US approach.<sup>31</sup> The pathway along  $z$  was divided into a sequence of overlapping “windows” approximately 7 Å wide.<sup>44</sup> Two consecutive windows overlapped by at least 2 Å. Up to eight windows were, thus, required to obtain the complete free energy profile characterizing the transfer of a pharmacologically active molecule across the water–dodecane interface. The solute was confined within each window by means of a harmonic restraining potential,  $\mathcal{U}_{\text{bias}}(z)$ . Furthermore, an appropriate biasing potential,  $\mathcal{U}'_{\text{bias}}(z)$ , was included to guarantee uniform sampling and, hence, uniform biased probabilities,  $\mathcal{P}_{\text{bias}}(z)$ , of finding the solute within the window of interest. The individual free energy curves per window,  $A(z)$ , were determined within a constant term  $A_0$ , from

$$A(z) = -k_B T \ln \mathcal{P}_{\text{bias}}(z) + \mathcal{U}_{\text{bias}}(z) + \mathcal{U}'_{\text{bias}}(z) + A_0 \quad (1)$$

Here,  $k_B$  is the Boltzmann constant and  $T$  the temperature. Depending upon the position of the solute along the  $z$ -direction and its nature, between 2 and  $9 \times 10^{-9}$  s of sampling were performed to ensure proper convergence. In all, a total simulation time of 19.7, 12.5, 20.4, and  $12.8 \times 10^{-9}$  s was necessary to investigate the transfer of antipyrine, caffeine, ganciclovir, and  $\alpha$ -D-glucose, respectively, across the water–dodecane interface. The significant length of the simulations—which does not necessarily translate into a sizable computational investment, considering the limited size of the system—can be rationalized by the requirement to sample those degrees of freedom orthogonal to the reaction coordinate, i.e., the distance separating the center of mass of the solutes from that of the dodecane phase. Moreover, a critical drawback of the US approach lies in the necessity to guess the shape of  $\mathcal{U}'_{\text{bias}}(z)$ , which can prove to be an intricate task for qualitatively new problems. As a result, additional sampling may be required to compensate for suboptimal estimates of the biasing potentials. It should be mentioned, however, that this difficulty can

be circumvented when using the promising adaptive force bias (AFB) algorithm,<sup>45</sup> which obviates the need to define  $\mathcal{U}'_{\text{bias}}(z)$  to guarantee a uniform distribution of  $\mathcal{P}_{\text{bias}}(z)$ . The complete free energy profiles were obtained by minimizing the deviation in the curvature of adjacent, individual curves. The error affecting the final free energies arises from two main contributions, namely (i) the statistical error at each point of the profiles, which can be inferred by dividing the simulation in each window into batches, over which a root-mean-square deviation is computed and (ii) the systematic error occurring when matching the individual curves to construct the complete free energy profile. It will be assumed that these contributions are uncorrelated.

An important aspect of the calculations reported here concerns the appropriateness of the charge distribution borne by the solute. As discussed above, net atomic charges have been derived from the electrostatic potential computed from a perturbed wave function,  $|\psi\rangle$ , using a continuum description of the surroundings. With a dielectric permittivity of 78.3, the fitted set of charges,  $\{q_k\}$ , is no longer characteristic of a low-pressure, gaseous state but of the bulk, aqueous medium. In essence, the polarity of the system has been exaggerated to account for the missing induction terms in the pairwise, additive description of the potential energy function. Whereas the charges  $\{q_k\}$  are ad hoc in the water phase of the interfacial system, they, however, correspond to an overestimated polarity in the nonpolar environment. This results in a positive, reversible work, referred to as distortion energy:<sup>46–51</sup>

$$\Delta A_{\text{distort}} = \langle \psi | \hat{\mathcal{H}}_0 | \psi \rangle - \langle \psi_0 | \hat{\mathcal{H}}_0 | \psi_0 \rangle \quad (2)$$

where  $\hat{\mathcal{H}}_0$  and  $|\psi_0\rangle$  are the unperturbed Hamiltonian and wave function. The corresponding set of charges will be referred to as  $\{q_{k,0}\}$ . The choice of point charges characteristic of the gas phase, rather than the nonpolar medium, lies in the choice of a united-atom model to describe the dodecane molecules,<sup>33</sup> wherein  $-\text{CH}_2-$  and  $-\text{CH}_3$  moieties do not carry a partial charge. The first term of eq 2 can be obtained by introducing the SCRf wave function,  $|\psi\rangle$ , into a standard self-consistent field (SCF) cycle, employing the nonperturbed Hamiltonian. The second one is simply the gas-phase Hartree–Fock energy.

Considering that  $\Delta A_{\text{distort}} > 0$  in the nonpolar phase, the corrected transfer free energy difference is now  $\Delta A_{\text{water} \rightarrow \text{oil}} =$



$A(\text{oil}) - A(\text{water}) - \Delta A_{\text{distort}}$ . The distortion energy, however, is not a constant, but clearly varies with  $z$ , thereby reflecting the smooth transition between the macroscopic permittivities of the polar and the nonpolar media. As a result, the adsorption free energy at the water–oil interface is equally affected by the variation of the charge distribution along the reaction coordinate. Conventionally, it was chosen to modify  $\{q_k\}$  into  $\{q_{k,0}\}$  following the behavior of  $\rho_{\text{water}}(z)$ , the density profile of water in the system, so that in the bulk dodecane phase, the appropriate set of charges is  $\{q_{k,0}\}$ .

**2.3. Experimental Determination of Partition Coefficients.** As a basis of comparison, water–dodecane partition coefficients were determined experimentally for a series of molecules, among which those examined in this contribution. Ganciclovir was obtained from the ASTRAZENECA compound collection, dodecane HPLC grade and 4-methyl-sulfonylacetophenone were purchased from ACROS ORGANICS, diazepam was purchased from SIGMA, 1-octanol HPLC grade and all other chemicals were purchased from Aldrich. The water–1-octanol and water–dodecane partition coefficients were determined employing the shake flask method. The organic phases, 1-octanol and dodecane, were presaturated by water. The phosphate buffer (0.1 M and pH 7) was prepared with organic solvent saturated water. The chemical compounds of interest were dissolved in the phosphate buffer, and an aliquot was kept as the reference for aqueous concentration before extraction. The organic solvent was then added, and the two phases were mixed vigorously during 1 h before being separated by centrifugation. The aqueous concentrations before and after partition were measured via HPLC. The  $\log_{10} P$  were calculated using the following expression:

$$\log_{10} P = \log_{10} \left( \frac{c_{\text{aq}}^b - c_{\text{aq}}^a}{c_{\text{aq}}^a} \frac{V_{\text{aq}}}{V_{\text{org}}} \right) \quad (3)$$

where  $c_{\text{aq}}^b$  and  $c_{\text{aq}}^a$  are, respectively, the concentrations in the aqueous phase before and after the extraction.  $V_{\text{aq}}$  and  $V_{\text{org}}$  are the volumes of the aqueous and the organic phases, respectively.

To obtain relevant  $\log_{10} P$  estimates, the aqueous concentrations before and after partition must be significantly different. The organic solvent/buffer ratio can, therefore, be adjusted at the beginning of the experiment up to a 100/1 ratio, the smallest volume corresponding to the phase in which the chemical compound is likely to be extracted. All  $\log_{10} P$  measurements were performed at least in triplicates.

### 3. Results and Discussion

Statistical simulations of the partitioning of organic molecules across the water–dodecane interface allows the estimation of transfer free energies, and hence, water–dodecane partition coefficients, referred to as  $\log_{10} P_{\text{wat-dod}}$ . To validate such calculations, it is possible to measure experimentally the water–dodecane partition coefficients of the molecules investigated here. The main difficulty of these measurements lies in the experimental conditions per se, incompatible with coefficients falling below  $-3$ . Water–oil  $\log_{10} P$  above  $+3$  can, however, be measured easily for ionizable compounds,<sup>52</sup> while raising conceptual difficulties in terms of MD simulations—the most problematic issue being the accurate treatment of long-ranged,  $1/r^2$ , charge–dipole interactions, together with the evolution of the charge distribution when the solute is translocated from the aqueous medium to the nonpolar one. Calculation of  $\log_{10} P_{\text{wat-dod}}$  based upon transfer free energies can easily overshoot the lower limit. Such is the case, for instance, of both ganciclovir and  $\alpha$ -D-glucose, the parti-

**Table 1.** Experimental Water–Octanol,  $\log_{10} P_{\text{wat-oct}}$ , and Water–Dodecane,  $\log_{10} P_{\text{wat-dod}}$ , Partition Coefficients of a Series of Prototypical Molecules Measured by Shake Flask<sup>a</sup>

molecule	$\log P_{\text{wat-dod}}$	$\log P_{\text{wat-oct}}$
antipyrene	-2.52	0.15
caffeine	-2.33	-0.09
ganciclovir	<-3.00	-2.07
$\alpha$ -D-glucose	<-3.00	-3.02
acetanilide	-1.76	1.13
acetophenone	0.94	1.56
acridine	2.32	2.98
anisole	2.06	2.11
anthranilamide	-2.72	0.32
benzamide	-2.67	0.67
benzenesulfonamide	-3.14	0.33
benzyl alcohol	-0.77	1.12
3-bromoquinoline	2.59	3.11
3-chlorophenol	-0.34	2.51
diazepam	1.49	2.87
4-(dimethylamino)antipyrene	-1.10	0.82
1-methylisatin	-0.90	0.63
4-methylsulfonylacetophenone	-1.56	0.33
nitrobenzene	1.43	1.84
oxindole	-1.95	1.07
phenol	-1.04	1.50
quinoxaline	0.51	1.35

<sup>a</sup> Values are given within an error of 0.10.

tion coefficient of which falls below  $-3$ . In contrast, the  $\log_{10} P_{\text{wat-dod}}$  of antipyrene and caffeine was measured reliably at  $-2.52$  and  $-2.33$ , respectively.

To estimate the  $\log_{10} P_{\text{wat-dod}}$  of ganciclovir and  $\alpha$ -D-glucose, it was postulated that partition coefficients between dodecane and water are necessarily related to those between 1-octanol and water. The partition coefficients in these two distinct environments were, therefore, measured for a series of prototypical compound, reported in Table 1. The  $\log_{10} P_{\text{wat-oct}}$  of ganciclovir and  $\alpha$ -D-glucose were found to be  $-2.07$  and  $-3.02$ , respectively. Differences in the partition coefficients, i.e.,  $\log_{10} P_{\text{wat-dod}} - \log_{10} P_{\text{wat-oct}}$ , were correlated with structural molecular descriptors chosen from a set of about 100 molecular descriptors taken from DRONE and involving either linear correlations or neural networks. From the behavior of  $\log_{10} P_{\text{wat-dod}} - \log_{10} P_{\text{wat-oct}}$ , extrapolated using these different models, in conjunction with the measured  $\log_{10} P_{\text{wat-oct}}$ ,  $\log_{10} P_{\text{wat-dod}}$  were inferred between  $-8.1$  and  $-5.1$  for ganciclovir and between  $-11.1$  and  $-7.6$  for  $\alpha$ -D-glucose. These two particular compounds are far in their chemical properties from the training set of molecules presented in Table 1, thus rationalizing the large differences observed between the models utilized and suggesting that unequivocal estimation of the  $\log_{10} P_{\text{wat-dod}}$  for these two compounds is a difficult task.

The free energy profiles for the four solutes are shown in Figure 3. From the onset, it can be seen that, except for  $\alpha$ -D-glucose, all the curves possess an interfacial minimum, highlighting the amphipathic character of these molecules and their propensity to remain near the interface.  $\alpha$ -D-Glucose is too hydrophilic and, therefore, unlikely to accumulate at the water–oil interface. On the basis of these free energy calculations, a partition coefficient can be inferred from the end points of the profiles, viz.,  $\log_{10} P_{\text{wat-dod}} = -\Delta A_{\text{wat-dod}}/2.3k_{\text{B}}T$ , where  $\Delta A_{\text{wat-dod}} = A(\text{dodecane}) - A(\text{water})$ . At first glance, the agreement between the computed quantities and the experimentally determined ones is noteworthy. For

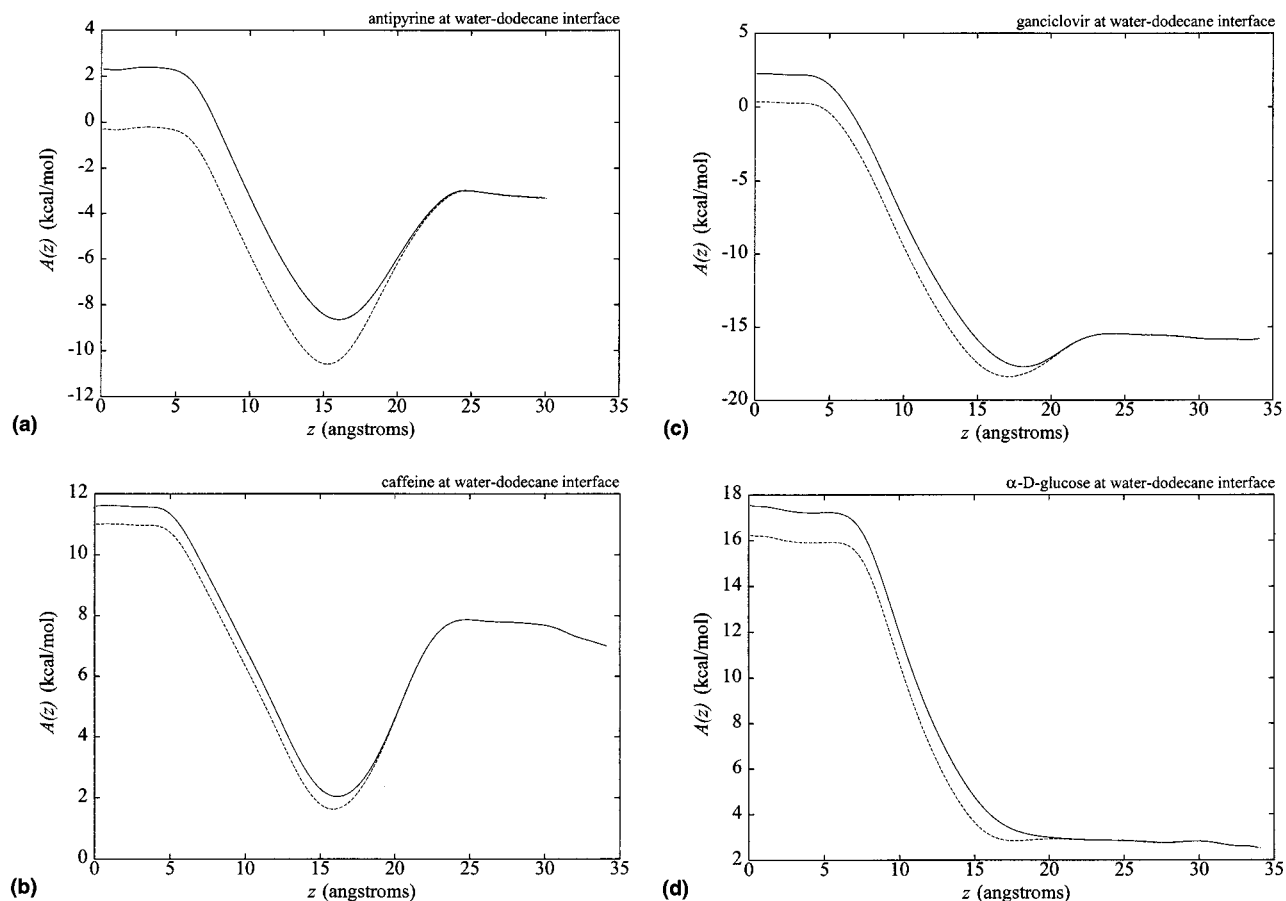


**Figure 3.** Transfer free energies of antipyrine, caffeine, ganciclovir, and  $\alpha$ -D-glucose across the water–dodecane interface: uncorrected profile (solid line) and profile incorporating the distortion energy,  $\Delta A_{\text{distort}}$  (dashed line).

**Table 2.** Transfer Free Energies<sup>a</sup> and Partition Coefficients of Small, Pharmacologically Relevant Solutes across the Water–Dodecane Interface Estimated from Statistical Simulations and Determined Experimentally

molecule	calculated			experimental <sup>b</sup>
	$\Delta A_{\text{wat-dod}}$	$\Delta A_{\text{adsorp}}$	$\log_{10} P_{\text{wat-dod}}$	$\log_{10} P_{\text{wat-dod}}$
antipyrine	$3.0 \pm 0.5$	$7.9 \pm 0.5$	-2.1	-2.5
caffeine	$3.8 \pm 0.6$	$6.4 \pm 0.6$	-2.7	-2.3
ganciclovir	$16.3 \pm 0.6$	$3.0 \pm 0.6$	-11.5	-8.1 to -5.1
$\alpha$ -D-glucose	$13.6 \pm 0.6$	$0.2 \pm 0.6$	-9.5	-11.1 to -7.6

<sup>a</sup> All free energies in kcal/mol. <sup>b</sup> Experimental estimates for ganciclovir and  $\alpha$ -D-glucose correspond to extrapolations, on account of the detectability threshold characteristic of the method utilized.

caffeine,  $\alpha$ -D-glucose, and antipyrine, the accord is within chemical accuracy (see Table 2). It should be noted, however, that for both ganciclovir and  $\alpha$ -D-glucose comparison with experimental measurements is more difficult considering the hydrophilic nature of the solutes.

For  $\alpha$ -D-glucose, the theoretical estimate falls within the bracket extrapolated from the actual, measured values. The case of ganciclovir is, however, somewhat more problematic, albeit the trend is reproduced qualitatively. A likely answer rationalizing the witnessed difference between experiment and simulations may lie in the choice of the potential energy function for the description of solute–solvent interactions. It should be emphasized that van der Waals parameters were taken from the general purpose AMBER all-atom force field,<sup>34</sup> which conceptually was not designed for small, organic

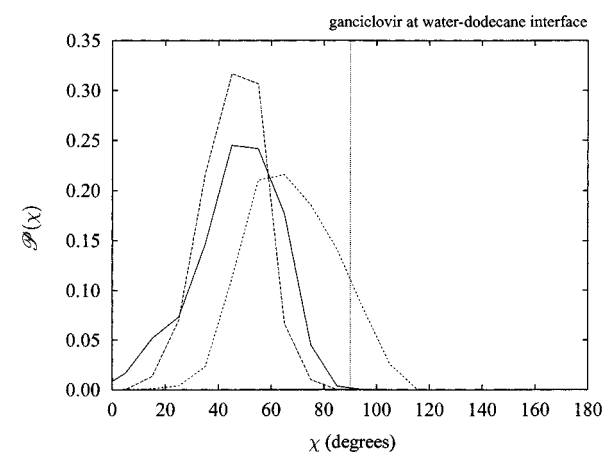


**Figure 4.** Probability distribution of angle  $\chi \equiv \text{N-C-O-C}$  in the flexible chain of ganciclovir, in water (short-dashed line), in dodecane (long-dashed line), and at the interface (solid line).

molecules but rather for biological macromolecules. In a limited number of instances, the selection of a particular type of atom was questionable, and the corresponding Lennard-Jones parameters might be less than optimal in the context of free energy calculations. Another difficulty is rooted in the flexibility of ganciclovir and possible conformational changes along  $z$ . Looking, however, at the probability distribution of angle  $\chi \equiv \text{N-C-O-C}$  reported in Figure 4, it would seem that the polar chain of ganciclovir does not undergo any peculiar transition and is somewhat more flexible in water than both in dodecane and at the

interface. The latter effect is marginal for the other torsional angles in the chain. In any event, it is worth noting that, whereas both antipyrine and caffeine correspond to an absorption coefficient of 100%, ganciclovir is only marginally absorbed, viz. 3.8%, in line with the observed trend.<sup>53,54</sup>

The statistical simulations reported here also highlight the paramount importance of electrostatic interactions in the estimation of transfer free energies of organic molecules from a polar environment to a non-polar one. Net atomic charges determined from an SCRF calculation<sup>35</sup> using a macroscopic permittivity of 78.3 account in an average fashion for the missing induction effects in the aqueous phase. Such sets of point charges are, however, inappropriate in the hydrophobic medium, as they exaggerate the polarity of the molecule in this environment. The profiles reported in Figure 3 indicate that the distortion energy can be appreciable<sup>46,51</sup> and can modulate substantially the overall free energies,  $\Delta A_{\text{wat-dod}}$ , and, thus, the partition coefficients,  $\log_{10} P_{\text{wat-dod}}$ . For instance, the dipole moment of antipyrine, using a permittivity of 1.0 and 78.3 is 6.9 and 8.9 D, respectively. This variation corresponds to  $\Delta A_{\text{distort}} = 2.6$  kcal/mol, which would yield an uncorrected partition coefficient of ca.  $-3.9$ , compared to the experimental value of  $-2.1$ . It is worth noting that the distortion energy not only affects transfer free energies but also the adsorption free energies. The latter are estimated from the one-dimensional profiles of Figure 3 as the difference between the free energy of the solute in the aqueous medium, viz. roughly speaking,  $z > 25$  Å, and that corresponding to the interfacial minimum, viz.  $z \approx 16$  Å.<sup>55</sup> A rapid inspection of these profiles demonstrate that, depending upon the nature of the solute, the correction described in eq 2 can alter the depth of the interfacial minimum. In the case of antipyrine, the adsorption free energy is lowered by approximately 2 kcal/mol. Interestingly enough, the same correction applied to  $\alpha$ -D-glucose leads to the appearance of a very small minimum, when the uncorrected profile showed a monotonic decrease of  $A(z)$  when the molecule is transferred from dodecane to water.

As already mentioned, the present results suggest that antipyrine and caffeine are better absorbed than ganciclovir, in good agreement with experimental measurements.<sup>53,54</sup> Their comparable  $\log_{10} P_{\text{wat-dod}}$ , viz.  $-2.5$  and  $-2.3$ , is considerably smaller than that of ganciclovir, viz.  $-7.3$ . Aside from the partition coefficients, the present statistical simulations also allow to investigate how these molecules of pharmacological interest behave at the water–dodecane interface. Both antipyrine and caffeine exhibit a large adsorption free energy,  $\Delta A_{\text{adsorp}}$ , equal to 7.9 and 6.4 kcal/mol. These significant adsorption minima are characteristic of amphipathic species, the dipole moment,  $\mu$ , of which is likely to interact favorably with the excess electric field created by the interface environment. It should be noted that only the  $z$ -component of the field,  $\mathcal{E}_z$ , collinear to the normal to the interface, is nonzero—the average, but not the instantaneous,  $x$ - and  $y$ -components being nil. The interaction of the field and the dipole moment borne by the pharmacologically relevant molecule results in an orientational anisotropy at the interface. This phenomenon can be appreciated by examining the prob-

ability distribution of angle  $\theta \equiv (\mu, \mathcal{E}_z)$ , expressed as

$$\mathcal{P}(\theta) = \frac{N_\theta}{N \sin \theta} \quad \text{and} \quad \sum_\theta \mathcal{P}(\theta) \sin \theta = 1 \quad (4)$$

in the bulk phases and in the interfacial environment. Here,  $N_\theta$  denotes the number of configurations for which  $(\mu, \mathcal{E}_z)$  is in the range  $\theta \pm \delta\theta$ .  $N$  is the total number of configurations.  $\mathcal{P}(\theta)$  is normalized to describe the probability of finding  $\mu$  in the same solid angles at different values of  $\theta$ . As can be observed in Figure 5, the role exerted by the interface on the orientational preference of the four solutes can vary significantly. In the case of antipyrine, orientation in the bulk phases is roughly isotropic with a slight tendency to align  $\mu$  parallel to  $\mathcal{E}_z$  in the aqueous environment. This effect is even more pronounced for caffeine and ganciclovir. In contrast, the interface appears to favor the perpendicular orientation of  $\mu$  with respect to the  $z$ -component of the excess electric field. This result is likely to stem from the fact that the most probable orientation of the dipole moment borne by water molecules is parallel to the interface, the excess electric field arising only from a slight asymmetry of their distribution.<sup>56,57</sup> The favorable interaction of  $\mu$  with the instantaneous  $x$ - and  $y$ -components of the field is particularly glaring in the example of caffeine, for which  $\mathcal{P}(\theta)$  follows a Gaussian distribution. Orientational anisotropy is more difficult to discern in the case of  $\alpha$ -D-glucose, considering that the interfacial minimum is less than  $k_B T$ , well within the error bar of the free energy calculation. Last, it is worth pointing out that, not too unexpectedly, antipyrine, when located at the water–dodecane interface, shows a conspicuous tendency to segregate its phenyl moiety in the nonpolar phase, while exposing its polar group to the aqueous medium. Similarly, ganciclovir buries its flexible polar chain in water and preserves at the same time partial hydration of its hydroxyl and amino groups.

#### 4. Conclusion

The determination of transfer free energies of a series of pharmacologically relevant small, organic molecules across the water–dodecane interface, using state-of-the-art free energy calculations, is reported. The accord with experiment is noteworthy, emphasizing the maturity of this methodology, now part of the modeler's toolkit, to tackle problems of both increased complexity and pertinence to the pharmaceutical world. From a technical point of view, the present calculations illustrate the necessity to account for missing induction effects, using, for instance, an implicit scheme, as was done here. Should a single set of net atomic charges be employed to model a solute transferred between two media of distinct permittivity, the inclusion of the distortion energy into the estimated free energy is a *sine qua non* condition to warrant accurate results.<sup>46,51</sup> Free energy calculations remain, however, costly, and, if targeted at the simple estimation of partition coefficients, are, at the present time, evidently less effective than bench experiments. Several models at various levels of sophistication have been proposed lately to determine partition coefficients rapidly, thereby allowing large sets of drugs to be screened—a key requirement for the pharmaceuti-

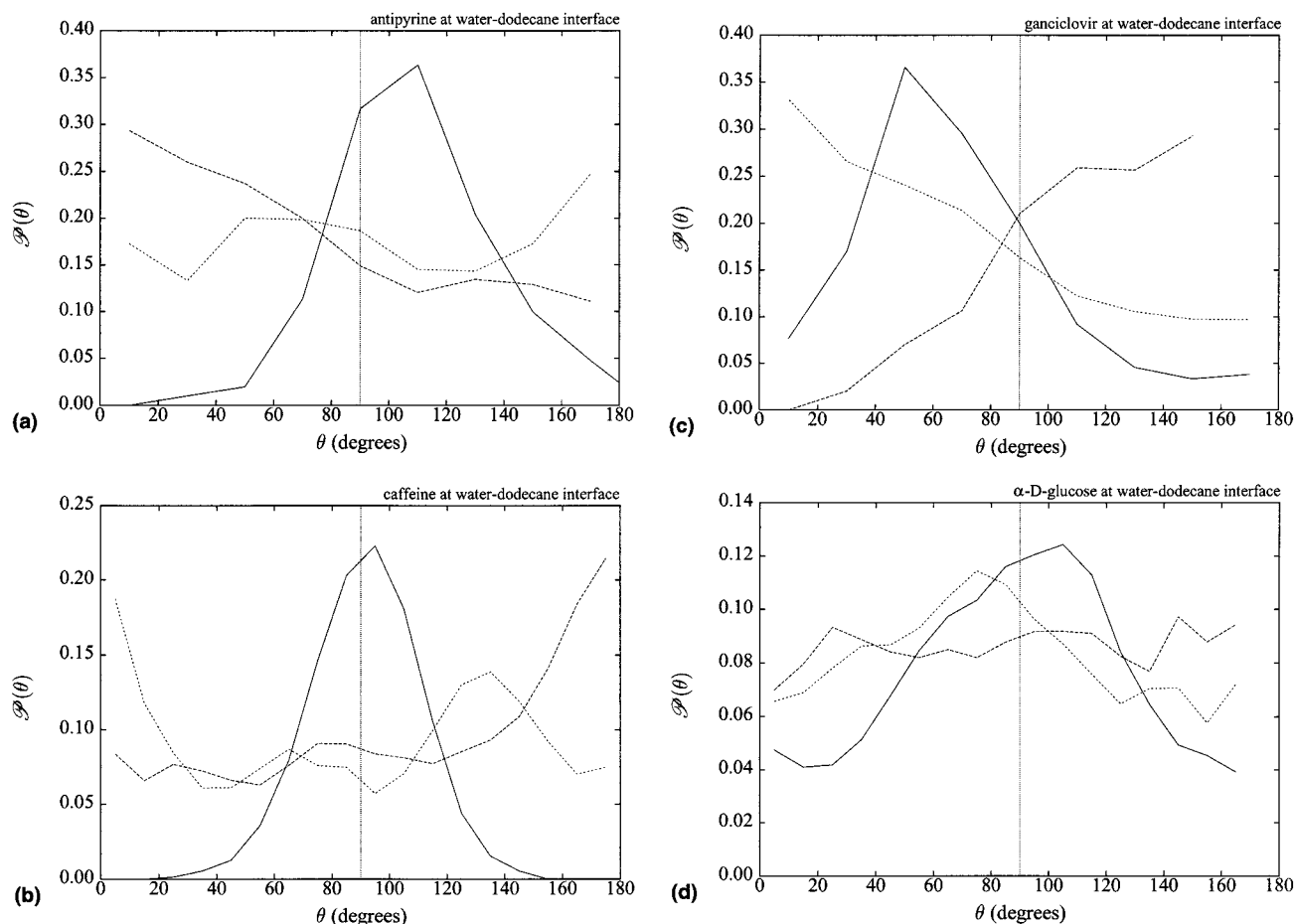


**Figure 5.** Probability distribution of angle  $\theta$  between the dipole moment of antipyrine, caffeine, ganciclovir, and  $\alpha$ -D-glucose and the  $z$ -component of the excess electric field, in water (short-dashed line), in dodecane (long-dashed line), and at the interface (solid line). Because the simulation cell involves two water–dodecane interfaces,  $0^\circ \leq 90^\circ$  and  $90^\circ \leq 180^\circ$  correspond alternatively to the polar and the nonpolar phase of the system.

cal industry.<sup>17–20</sup> Among the most promising, continuum generalized Born/surface area (GB/SA) calculations have proven to be particularly powerful for estimating water–1-octanol partition coefficients accurately, significantly faster than the more classical free energy perturbation (FEP) methodology.<sup>17,58</sup> Equally promising are those approaches relying upon the linear response approximation coupled to statistical simulations.<sup>19,59,60</sup> These methods aimed at the fast, qualitative estimation of free energy changes, however, often include a heuristic component in their conception. The latter generally appears in the form of a training set, which calls into question the validity of the approach for qualitatively different compounds than those incorporated in the training set. It can be argued that, if use is made of a well-parametrized potential energy function and appropriate sampling protocols, first-principles free energy calculations should prove to be more consistent in their estimations of partition coefficients. More importantly, the classical computations performed here offer more than a simple  $\log_{10} P$ . By scrutinizing the complete free energy profile in the direction normal to the interface, the true physical chemistry of the solute at an aqueous interface is unraveled and brought to light. Depending upon the chemical nature of the molecule investigated, the generated free energy profiles can exhibit interfacial minima that correspond to the tendency of the chemical species to accumulate at the interface. This unique effect

cannot be predicted from the sole knowledge of the properties characteristic of the molecule in the bulk phases. It is envisioned that interfacial activity might play an underlying role in the propensity of a drug to cross the biological membrane, and only statistical simulations are capable of providing a convincing answer. In the relevant case of general anesthesia by inhaled anesthetics, for instance, similar calculations have refuted the hitherto accepted Meyer–Overton hypothesis<sup>61</sup> and suggested that general anesthesia is an interfacial phenomenon.<sup>62–64</sup> Clearly, such conclusions could not have been reached in the sole light of simple partition coefficients that do not supply any information about the possible interaction of the molecule of interest with the interface.

**Acknowledgment.** We are indebted to ASTRAZENECA, France, for supporting the present project. The Centre Charles Hermite (CCH), Vandœuvre-lès-Nancy, France, and the CINES, Montpellier, France, are gratefully acknowledged for provision of generous amounts of CPU time on their SGI Origin 2000.

## References

- (1) Carrupt, P.; Testa, B.; Gaillard, P. Computational approaches to lipophilicity: Methods and applications. In *Reviews in Computational Chemistry*; Lipkowitz, K., Boyd, D. B., Eds.; VCH: New York, 1997; Vol. 11, pp 241–345.



- (2) Hansch, C.; Dunn, W. J., III. Linear relationships between lipophilic character and biological activity of drugs, *J. Pharm. Sci.* **1972**, *61*, 1–19.
- (3) Martin, Y. C. *Quantitative drug design*; Marcel Dekker: New York, 1978.
- (4) Ong, S. W.; Liu, H. L.; Pidgeon, C. Immobilized artificial membrane chromatography: Measurements of membrane partition coefficient and predicting drug membrane permeability. *J. Chromatogr.* **1996**, *728*, 113–128.
- (5) Lipinski, C. A.; Lombardo, F.; Dominy, B. W.; Feeney, P. J. Experimental and computational approaches to estimate solubility and permeability in drug discovery and development settings. *Adv. Drug Delivery Rev.* **1997**, *23*, 3–25.
- (6) Mouritsen, O. G.; Jørgensen, K. A new look at lipid-membrane structure in relation to drug research. *Pharm. Res.* **1998**, *15*, 1507–1519.
- (7) Bassolino-Klimas, D.; Alper, H. E.; Stouch, T. R. Drug-membrane interactions studied by molecular dynamics simulation: Size dependence of diffusion. *Drug Des. Discovery* **1996**, *13*, 135–141.
- (8) Marrink, S. J.; Berendsen, H. J. C. Permeation process of small molecules across lipid membranes studied by molecular dynamics. *J. Phys. Chem.* **1996**, *100*, 16729–16738.
- (9) Tu, K.; Tarek, M.; Klein, M. L.; Scharf, D. Effects of anesthetics on the structure of a phospholipid bilayer: Molecular dynamics investigation of halothane in the hydrated liquid crystal phase of dipalmitoylphosphatidylcholine. *Biophys. J.* **1998**, *75*, 2123–2134.
- (10) Pohorille, A.; Wilson, M. A.; Schweighofer, K.; New, M. H.; Chipot, C. Interactions of membranes with small molecules and peptides. In *Theoretical and Computational Chemistry—Computational Molecular Biology*; Leszczynski, J., Ed.; Elsevier: The Netherlands, 1999; Vol. 8, pp 485–535.
- (11) Tieleman, D. P.; Marrink, S. J.; Berendsen, H. J. C. A computer perspective of membranes: Molecular dynamics studies of lipid bilayer systems. *Biochim. Biophys. Acta* **1997**, *1331*, 235–270.
- (12) Leo, A.; Hansch, C.; Elkins, D. Partition coefficients and their uses. *Chem. Rev.* **1971**, *71*, 525–616.
- (13) Leo, A. Calculating log P(oct) from structures. *Chem. Rev.* **1993**, *93*, 1281–1306.
- (14) Jørgensen, W. L.; Briggs, J. M.; Contreras, M. L. Relative partition coefficients for organic solutes from fluid simulations. *J. Phys. Chem.* **1990**, *94*, 1683–1686.
- (15) Essex, J. W.; Reynolds, C. A.; Richards, W. G. Theoretical determination of partition coefficients. *J. Am. Chem. Soc.* **1992**, *114*, 3634–3639.
- (16) Orozco, M.; Colominas, C.; Luque, F. J. Theoretical determination of the solvation free energy in water and chloroform of the nucleic acid bases. *Chem. Phys.* **1996**, *9*, 209–678.
- (17) Best, S. A.; Merz, K. M., Jr.; Reynolds, C. H. Free energy perturbation study of octanol/water partition coefficients: Comparison with continuum GB/SA calculations. *J. Phys. Chem. B* **1999**, *103*, 714–726.
- (18) Torrens, F. Universal organic solvent–water partition coefficient model. *J. Chem. Inf. Comput. Sci.* **2000**, *40*, 236–240.
- (19) Duffy, E. M.; Jørgensen, W. L. Prediction of properties from simulations: Free energies of solvation in hexadecane, octanol and water. *J. Am. Chem. Soc.* **2000**, *122*, 2878–2888.
- (20) Curutchet, C.; Orozco, M.; Luque, F. J. Solvation in octanol: Parametrization of the continuum MST model. *J. Comput. Chem.* **2001**, *22*, 1180–1193.
- (21) DeBolt, S. E.; Kollman, P. A. Investigation of structure, dynamics, and solvation in 1-octanol and its water-saturated solution: Molecular dynamics and free energy perturbation studies. *J. Am. Chem. Soc.* **1995**, *117*, 5316–5340.
- (22) Pohorille, A.; Wilson, M. A.; Chipot, C. Interaction of alcohols and anesthetics with the water-hexane interface. A molecular dynamics study. *Prog. Colloid Polym. Sci.* **1997**, *103*, 29–40.
- (23) Grès, M. C.; Julian, B.; Bourrié, M.; Meunier, V.; Roques, C.; Berger, M.; Boulenc, X.; Berger, Y.; Fabre, G. Correlation between oral drug absorption in humans, and apparent drug permeability in TC-7 cells, a human epithelial intestinal cell line: Comparison with the parental Caco-2 cell line. *Pharm. Res.* **1998**, *15*, 726–733.
- (24) Tanaka, H.; Mizojiri, K. Drug–protein binding and blood-brain permeability. *J. Pharm. Exp. Ther.* **1999**, *288*, 912–918.
- (25) Hilgendorf, C.; Spahn-Langguth, H.; Regårdh, C. G.; Lipka, E.; Amidon, G. L.; Langguth, P. Caco-2 versus Caco-2/HT29-MTX co-cultured cell lines: Permeabilities via diffusion, inside- and outside-directed carrier-mediated transport. *J. Pharm. Sci.* **2000**, *89*, 63–75.
- (26) Mark, A. E. Free Energy Perturbation Calculations. In *Encyclopedia of computational chemistry*; Schleyer, P. v. R., Allinger, N. L., Clark, T., Gasteiger, J., Kollman, P. A., Schaefer, H. F., III, Schreiner, P. R., Eds.; Wiley and Sons: Chichester, 1998; Vol. 2, pp 1070–1083.
- (27) Chipot, C.; Pearlman, D. A. Free energy calculations. The long and winding gilded road. *Mol. Simul.* (in press).
- (28) Wohnsland, F.; Faller, B. High-throughput permeability pH profile and high-throughput alkane-water log P with artificial membranes. *J. Med. Chem.* **2001**, *44*, 923–930.
- (29) Leahy, D.; Taylor, P.; Wait, A. Model solvent systems for QSAR. Part I. Propylene glycol dierperlgonate (PGDP). A new standard solvent for use in partition coefficient determination. *Quant. Struct.-Act. Relat.* **1989**, *8*, 17–31.
- (30) Torrie, G. M.; Valleau, J. P. Monte Carlo free energy estimates using non-Boltzmann sampling: Application to sub-critical Lennard-Jones fluids. *Chem. Phys. Lett.* **1974**, *28*, 578–581.
- (31) Torrie, G. M.; Valleau, J. P. Nonphysical sampling distributions in Monte Carlo free energy estimation: Umbrella sampling. *J. Comput. Phys.* **1977**, *23*, 187–199.
- (32) Jørgensen, W. L.; Chandrasekhar, J.; Madura, J. D.; Impey, R. W.; Klein, M. L. Comparison of simple potential functions for simulating liquid water. *J. Chem. Phys.* **1983**, *79*, 926–935.
- (33) Jørgensen, W. L.; Madura, J. D.; Swenson, C. J. Optimized potential energy functions for liquid hydrocarbons. *J. Am. Chem. Soc.* **1984**, *106*, 6638–6646.
- (34) Junmei, W.; Cieplak, P.; A. Kollman P. How well does a restrained electrostatic potential (RESP) model perform in calculating conformational energies of organic and biological molecules? *Theor. Chim. Acta* **2000**, *21*, 1049–1074.
- (35) Cramer, C. J.; Truhlar, D. G. Implicit solvation models: Equilibria, structure, spectra, and dynamics. *Chem. Rev.* **1999**, *99*, 2161–2200.
- (36) Rivaill, J. L.; Rinaldi, D. A quantum chemical approach to dielectric solvent effects in molecular liquids. *Chem. Phys.* **1976**, *18*, 233–242.
- (37) Rinaldi, D. Lamé's functions and ellipsoidal harmonics for use in chemical physics. *Comput. Chem.* **1982**, *6*, 155–160.
- (38) Reynolds, C. A.; Essex, J. W.; Richards, W. G. Atomic charges for variable molecular conformations. *J. Am. Chem. Soc.* **1992**, *114*, 9075–9079.
- (39) Allen, M. P.; Tildesley, D. J. *Computer Simulation of Liquids*; Clarendon Press: Oxford, 1987.
- (40) Ryckaert, J.; Ciccotti, G.; Berendsen, H. J. C. Numerical integration of the Cartesian equations of motion for a system with constraints: Molecular dynamics of *n*-alkanes. *J. Comput. Phys.* **1977**, *23*, 327–341.
- (41) Andrea, T. A.; Swope, W. C.; Andersen, H. C. The role of long-ranged forces in determining the structure and properties of liquid water. *J. Chem. Phys.* **1983**, *79*, 4576–4584.
- (42) Brooks, C. L., III; Pettitt, B. M.; Karplus, M. Structural and energetic effects of truncated long-ranged interactions in ionic and polar fluids. *J. Chem. Phys.* **1985**, *83*, 5897–5908.
- (43) Barker, J. A.; Watts, R. O. Monte Carlo studies of the dielectric properties of water-like models. *Mol. Phys.* **1973**, *26*, 789–792.
- (44) Valleau, J. P.; Card, D. N. Monte Carlo estimation of the free energy by multistage sampling. *J. Chem. Phys.* **1972**, *57*, 5457–5462.
- (45) Darve, E.; Pohorille, A. Calculating free energies using average force. *J. Chem. Phys.* **2001**, *115*, 9169–9183.
- (46) Luque, F. J.; Bofill, J. M.; Orozco, M. New strategies to incorporate the solvent polarization in self-consistent reaction field and free energy perturbation simulations. *J. Chem. Phys.* **1995**, *103*, 10183–10191.
- (47) Ángyán, J. G. Comment on “New strategies to incorporate the solvent polarization in self-consistent reaction field and free energy perturbation simulations” [*J. Chem. Phys.* **1995**, *103*, 10183–10191]. *J. Chem. Phys.* **1997**, *107*, 1–3.
- (48) Luque, F. J.; Orozco, M. Semiclassical-continuum approach to the electrostatic free energy of solvation. *J. Phys. Chem. B* **1997**, *101*, 5573–5582.
- (49) Luque, F. J.; Bofill, J. M.; Orozco, M. Response to Comment on “New strategies to incorporate the solvent polarization in self-consistent reaction field and free-energy perturbation simulations” [*J. Chem. Phys.* **1997**, *107*, 1–3]. *J. Chem. Phys.* **1997**, *101*, 5573–5582.
- (50) Orozco, M.; Luque, F. J. Generalized linear response approximation in discrete methods. *Chem. Phys. Lett.* **1997**, *265*, 473–480.
- (51) Chipot, C. Transfer free energies of small, organic solutes across the water liquid/vapor interface. Unpublished results, 2001.
- (52) Takács-Novák, K.; Avdeef, A. Interlaboratory study of log P determination by shake-flask and potentiometric methods. *J. Pharm. Biomed. Anal.* **1996**, *14*, 1405–1413.
- (53) Wessel, M. D.; Jurs, P. C.; Tolan, J. W.; Muskal, S. M. Prediction of human intestinal absorption of drug compounds from molecular structure. *J. Chem. Inf. Comput. Sci.* **1998**, *38*, 726–735.
- (54) Agatonovic-Kustrin, S.; Beresford, R.; Pauzi, A.; Yusof, M. Theoretically-derived molecular descriptors important in human intestinal absorption. *J. Pharm. Biomed. Anal.* **2001**, *25*, 227–237.
- (55) Pohorille, A.; Benjamin, I. Molecular dynamics of phenol at the liquid–vapor interface of water. *J. Chem. Phys.* **1991**, *94*, 5599–5605.



- (56) Pohorille, A.; Wilson, M. A. Reaction dynamics in clusters and condensed phases. In *The Jerusalem symposia on quantum chemistry and biochemistry*; Jortner, J., Levine, R. D., Pullman, B., Eds.; Kluwer: Dordrecht, 1993; Vol. 26, p 207.
- (57) Pohorille, A.; Wilson, M. A. Excess chemical potential of small solutes across water-membrane and water-hexane interfaces. *J. Chem. Phys.* **1996**, *104*, 3760–3773.
- (58) Jean-Charles, A.; Nicholls, A.; Sharp, K.; Honig, B.; Tempczyk, A.; Hendrickson, T. F.; Still, W. C. Electrostatic contributions of solvation energies: Comparison of free energy perturbation and continuum calculations. *J. Am. Chem. Soc.* **1991**, *113*, 1454–1455.
- (59) Åqvist, J.; Medina, C.; Samuelsson, J. E. A new method for predicting binding affinity in computer-aided drug design. *Protein Eng.* **1994**, *7*, 385–391.
- (60) Åqvist, J. Calculation of absolute binding free energies for charged ligands and effects of long-range electrostatic interactions. *J. Comput. Chem.* **1996**, *17*, 1587–1597.
- (61) Overton, E., *Studien über die Narkose zugleich ein Betrag zur allgemeinen Pharmakologie*; Verlag von Gustav Fischer: Jena, 1901.
- (62) Koblin, D. D.; Chortkoff, B. S.; Laster, M. J.; Eger, E. I.; Halsey, M. J.; Ionescu, P. Polyhalogenated and perfluorinated compounds that disobey the Meyer-Overton hypothesis. *Anesth. Analg.* **1994**, *79*, 1043–1048.
- (63) Chipot, C.; Wilson, M. A.; Pohorille, A. Interactions of anesthetics with the water-hexane interface. A molecular dynamics study. *J. Phys. Chem. B* **1997**, *101*, 782–791.
- (64) Pohorille, A.; Wilson, M. A.; New, M. H.; Chipot, C. Concentrations of anesthetics across the water-membrane interface; The Meyer-Overton hypothesis revisited. *Toxicol. Lett.* **1998**, *100*, 421–430.

JM010289A